FLY ASH COATED CHITOSAN AS EFFICIENT ADSORBENT FOR REMOVAL OF HEAVY METAL IONS FROM WATERS AND WASTEWATERS

Agnieszka Adamczuk, Dorota Kołodyńska*

Department of Inorganic Chemistry, Faculty of Chemistry,
Maria Curie Skłodowska University, Maria Curie Skłodowska Sq. 2, 20-031 Lublin, Poland.

Abstract

The aim of the paper was to study the effectiveness of Cu(II) removal onto fly ash (FAI) and fly ash coated by chitosan (FAICS). The changes in the morphology and physicochemical parameters of FAI activated at different temperatures were also investigated in order to optimize the modification process.

The obtained composite was characterized using the FTIR, SEM, BET and XRD methods. The following parameters such as initial concentration, pH, contact time, temperature and sorbent dosage were taken into account in order to evaluate its applicability in Cu(II) ions removal. The process kinetics was described using the pseudo first order, pseudo second order and intraparticle diffusion models. The Langmuir and Freundlich isotherm models were applied for analyzing experimental sorption equilibrium data. The thermodynamic parameters such as enthalpy, entropy and free energy of process were determined.

The results showed the highest efficiency in the case of sorption of Cu(II) onto FAICS compared with FAI. The obtained results were well described by the pseudo second order model. The adsorption data were well fitted with the Langmuir model. On this basis the maximum adsorption capacity were equal to 30.58 mg/g for FAI, 34.92 mg/g for FAI-973 and 34.36 mg/g for FAICS-973. It was also revealed that the process is spontaneous, favourable and endothermic in nature.

The proposed method of Cu(II) removal from aqueous solution can be readily used in practice taking into account efficiency and cost.

***Keywords*:** fly ash, chitosan, hybrid materials, adsorption, copper,

* Corresponding author: Tel.: +48 81 5375770; Fax:+48 81 5333348
E-mail address: kolodyn@poczta.onet.pl (D. Kołodyńska)

1. Introduction

Fly ash is a residue derived from combustion of coal in furnaces of thermal power plant. The use of poor quality coal with low calorific value resulted in large amount of fly ash after combustion. According to World Coal Association the total world coal production reached a record level of 7822 mln tons in 2013 (0.4% more than in 2012) [1]. As the European Coal Combustion Products Association reports [2] about 31 mln tons of fly ash was produced in Europe in 2010. Fly ash is one of the most widely used waste product in practice. According to the United States Environmental Protection Agency the main benefits of reusing this materials are lower greenhouse gas emissions, reducing the use of original resources and cost of fly ash disposal as well as improving strength and durability of the obtained sorbents used in the environmental protection [3].

Chemical and mineralogical compositions as well as physicochemical properties of fly ash depend on geochemical origin and calorific capacity of coal. The final structure of fly ash is also dependent on the variety of material parameters including water content, particle size, degree of amorphicity [4]. These parameters decided about the contents of glass and minerals in fly ash. The mineral composition of coal is of a wide variety and it is associated with the minerals presented in soil. The major minerals in fly ash are quartz (80% of fly ash) [5], mullite ($Al_6Si_2O_{13}$) and hematite (Fe_2O_3) [6]. The results obtained by Sztekler et al. [7] suggest that the main components of fly ash are SiO_2, Al_2O_3, Fe_2O_3 and CaO as well as MgO, Na_2O, K_2O and trace components such as TiO_2, P_2O_5, Mn_2O_5, PbO, NiO, CuO, ZnO, CdO as well as unburnt carbon. According to the American Society for Testing Materials (ASTM) [8], fly ashes which contain more than 70% of SiO_2, Al_2O_3 and Fe_2O_3 are classified as class F. In this class quartz or cristobalite, mullite, hematite, magnetite, lime, calcium sulfates (most of them - except alkali sulphates are embedded in the glass) can be distinguished [9]. It is well known that calcium aluminates, calcium silicates and calcium aluminosilicates begin to create at a temperature lower than 1273 K, whereas mullite is formed at higher temperatures [9]. This confirms that the conditions of combustion (temperature, pressure, type of emission control devices) also have great influence on fly ash composition as reported in [10, 11].

In order to change surface area, size of pores and crystalline structure as well as surface groups of fly ash it can be chemically and physically modified [12, 13]. One of the most popular methods of activation of fly ash is using high temperature [14,15]. The surface area and pores are created when gaseous products are liberated while heating [16, 17]. Temuujin et al. [18] reported that calcination caused approximately a 3% decrease of the amorphous component and increase the crystalline phases (mullite and hematite) of the fly ash. It was also suggested that at high temperature new crystalline phases with modifying siloxane groups (Si-O-Si) and different forms of silanol groups on fly ash surface are formed.

In the literature there are several papers on chitosan used for modification of fly ash. It causes an increase of adsorption capacity and improves the selectivity towards different pollutants from waters and wastewaters [19,20]. Chitosan is a popular biosorbent used to remove heavy metal ions from aqueous solutions [21-24]. It is a (1-4)-linked hetero polysaccharide consisting of 2-acetamido-2-deoxy-b-D-glucopyranose and 2-amino-2-deoxy-b-D-glucopyranose derived from chitin[(1-4)-linked 2-acetamido-2-deoxy-b-D-glucopyranose] [25]. The degree of deacetylation is an important parameter employed to differentiate chitin from chitosan [26]. It influences on the physicochemical properties of chitosan such as chain conformation, solubility, electrostatic properties [27]. Chitosan is insoluble in water, organic solvents and aqueous bases and it is soluble in acidic media such as acetic, phosphoric, nitric, hydrochloric, perchloric acids except sulfuric one [28,29]. Due to its biodegradability and biocompatibility chitosan is widely used e.g. in medicine and pharmacy [30], food [31], cosmetics [32], pulp and paper [33] and agriculture [34] industry.

The studies report the effective way for fly ash modification based on applicability of chitosan. However, to the authors' best knowledge, very few papers can be found in the literature that investigate fly ash coated by chitosan for removal of heavy metal ions. Therefore more information is still needed for better understanding of the adsorption behaviour of different heavy metal ions on the sorbent obtained by the proposed method. In the first stage fly ash was thermally activated at different temperatures (373-1173 K) and then modified by chitosan. The obtained sorbent was tested and evaluated for Cu(II) removal. The effects of activation temperature change were studied in order to optimize the modification process. The influence of parameters such as initial concentration, pH, contact time, temperature and adsorbent dosage was tested to optimize the sorption effectiveness of heavy metals ions from different industrial streams.

2. Materials and Methods

2.1. Materials

The coal fly ash (denoted as FAI) used in this study was collected from the Heat and Power Generating Plant Kozienice, Poland. According to ASTM [8] the material used in these studies is classified as class F because it contained less than 10% of CaO and more than 70% of the three main components SiO_2, Al_2O_3 and Fe_2O_3. Chitosan (denoted as CS) in the form of powder was supplied by Sigma-Aldrich (degree of deacetylation 76%, viscosity 261 cP, molecular mass 3.52×10^5 kDa). $CuSO_4\cdot5H_2O$ was used as a source of Cu(II) ions. The working stock solution was prepared by dissolving this salt in deionized water. The solution pH was adjusted by adding a small amount of 0.1 M NaOH and 0.1 M H_2SO_4. Additionally, NaCl and acetic acid were purchased from POCH (Poland). All the reagents used were of analytical grade.

2.2. Preparation of the adsorbent

Fly ash was thermally activated in a muffle furnace at 373, 773, 973, 1173 K for 1h and sieved. The obtained samples were denoted as FAI-373, FAI-773, FAI-973, FAI-1173. Chitosan was used in the experiments without further pretreatment. The chitosan solution was prepared by dissolving chitosan in acetic acid. Complete dissolution was achieved by continuous agitation using a magnetic stirrer at 1000 rpm for 24 h at room temperature. The activated fly ash was added to the chitosan solution (the ratios of fly ash to chitosan was 4:1). The mixture was adjusted to pH 9 with 5% NaOH solution and stirred for 30 min. In the next step the sorbent was filtered and washed with distilled water until pH of supernatant was neutral. The obtained material was dried in an oven at 323 K for 48 h and then sieved. The procedure was used for all activated fly ash and the obtained sorbents were abbreviated as FAICS-373, FAICS-773, FAICS-973, FAICS-1173 according to the activation temperature.

2.3. Kinetic and adsorption test

To examine kinetic parameters 20 cm^3 of the Cu(II) solution (pH=4.0) at the concentration 1×10^{-3} M-3×10^{-3} M. was added to 0.2 g of sorbent (shaking speed 180, temperature 293 K). The samples were removed and filtered at different time intervals from 1 to 180 min and the concentration of Cu(II) was determined.

During the investigations of the equilibrium adsorption isotherm 20 cm^3 solution (pH=4.0) of Cu(II) at the concentration 1×10^{-3} M-2.5×10^{-2} M was added to 0.2 g of sorbent (shaking speed 180, shaking time 180 min, temperature from 293 K to 333 K). After this the solution was filtered and the amount of Cu(II) was determined.

Tests of Cu(II) adsorption onto sorbent at different dosages 0.05-0.3 g were made at the initial concentrations 1×10^{-3} M-3×10^{-3} M. 20 cm^3 of solution (pH=4.0) was added to a suitable dosage of sorbent and shaken for 180 min with the shaking speed 180 rpm at 293 K. Then the samples were filtered and the concentration of Cu(II) ions was analyzed as previously.

2.4. Calculations

The rate of Cu(II) ions sorption is expressed as percentage of the amount of metal ions adsorbed after a certain time related to that required for the state of equilibrium. It can be described as follows:

$$S\% = \frac{(c_0 - c_e)}{c_0} \times 100\% \quad (1)$$

The sorbent phase concentrations of metal ions at equilibrium, q_e (mg/g) and at time t, q_t (mg/g) were obtained according to the following equations:

$$q_e = (c_0 - c_e) \times \frac{V}{m} \quad (2)$$

$$q_t = (c_0 - c_t) \times \frac{V}{m} \quad (3)$$

where: c_0 is the initial concentration of metal ion in the aqueous phase (mg/dm^3); c_t is the concentration of metal ion in the aqueous phase at time t (mg/dm^3); c_e is the concentration of metal ion in the aqueous phase at equilibrium (mg/dm^3); V is the volume of the solution (dm^3); m is the mass of the sorbent (g).

2.5. Analytical methods

The studies were carried out by the static method. The samples were shaken using the laboratory shaker type 357 (Elpin Plus). The pH was measured using a pH meter (Elmetron).

The concentration of Cu(II) ions was determined by AAS (atomic absorption spectroscopy) method using a spectrometer SpectrAA-FS 240 (Varian), which was equipped with a deuterium lamp, background correction, hollow cathode lamp for Cu and an air-acetylene burner. The amount of Cu(II) ions adsorbed was calculated based on the difference in their initial and final concentrations.

The measurement of specific surface area and average pore diameter was made using the BET (Brunauer, Emmett, Teller) instrument ASAP 2405 (Micrometrics Inc.). Scanning electron microscopy images were obtained Quanta 3D FEG microscope (FEI). Fourier transform infrared spectra of chitosan, fly ash and composite were obtained using the attenuated total reflectance technique (FTIR-ATR) and measured with a FTIR Carry 630 spectrometer (Agilent Technologies). The X-ray phase analysis (XRD) was made by the powder method using an X-ray diffractometer Philips X'pert APD (Panalytical) with a goniometer PW 3020 and Cu lamp a well as a graphite monochromator. The analyses were made at an angle 5-65 2θ. The pH of the point of zero charge pH_{zpc} was measured using the pH drift method [35]. The pH of the sorbent in 0.01 M NaCl solution was adjusted between 2 and 12 by adding 0.1 M NaOH and 0.1 M H_2SO_4. 0.2 g of the adsorbent was added to 50 cm^3 of the solution and after 24 h the final pH was measured.

3. Results

3.1. Characterization of the adsorbent

Physicochemical properties of FAI (chemical and mineral composition) and CS (deacetylation degree, chemical composition, molecular mass etc.) have the main influence on heavy metal ions sorption onto fly ash and fly ash coated by chitosan. The results of analysis of chemical composition of FAI presented in the previous paper [36] showed that basic components of fly ash are Al_2O_3 (27.50%) and SiO_2 (49.70%) as well as Fe_2O_3 (5.9%), calcium oxide CaO (4.59%), magnesium oxide MgO (3.09%), potassium oxide K_2O (2.98%) , titanium oxide TiO_2 (1.20) and sulphur defined as SO_3 (1.00). The analysis of chemical composition and physicochemical properties of CS showed that Ca, Mg, Na and K are basic components.

As follows from SEM analysis (Figs.1a-d) FAI and FAICS particles contained dense or spheres of different size and some unshaped fragments of unburned carbon. It can be also seen some of the smaller particles which were adhered on bigger ones.

Ricou-Hoeffer et al. reported [37] that the compounds containing silicon, silica oxide and calcium silicate hydrate are expected to play the most significant role in removal of metal ions. What is more, aluminosilicate compounds can also be involved in the adsorption phenomena through a SiO bond with metallic ions according to the scheme:

$$\equiv SiOH + OH^- \rightleftarrows \equiv SiO^- + H_2O \quad (4)$$

$$2(\equiv SiO\text{-}) + M^{2+} \rightleftarrows (\equiv SiO^-)_2 \ldots M^{2+} \quad (5)$$

Equilibrium (4) is observed when pH of the solution is above that pH of point of zero charge. Chitosan's amino groups can be also involved in the adsorption:

$$2{-}NH_2 + M^{2+} \rightleftarrows (-NH_2)_2M \quad (6)$$

It is worth mentioning that the investigated fly ash contained about 6% of Fe_2O_3, which can also be responsible for the Cu(II) ions removal.

It is well known that at solution pH values lower than that required for attaining the pH_{zpc}, the sites become protonated and an excess positive charge develops on the surface (for example, the oxides behave as a Brönsted acid or an anion exchanger). However, at pH values higher than the pH_{zpc}, the oxides behave as a Brönsted base or a cation exchanger. As follows from the literature data pH_{pzc} of SiO_2, α-Al_2O_3 and α-Fe_2O_3 was 2, 9.1 and 6.7, respectively [38]. At pH<pH_{pzc}, the surface of FAI had a net positive charge, while at pH>pH_{pzc} the surface had a net negative charge. In Figs.2a-b the results of pH drift method for determination of pH_{zpc} are presented. It was found that pH_{pzc} of FAI is equal to 6.5. However, after modification it is equal to 7.8 and do not change after thermal modification. It can be assumed that the

negative charge of active site on the surface of the FAICS allows metal ions or eventually metal hydroxides to be adsorbed at the surface.

The results of measurement of specific surface area and average pore diameter are presented in Table 1. All studied sorbents have the average pore diameter smaller than 50 nm which according to the International Union of Pure and Applied Chemistry (IUPAC) classification of pores [39] implies the presence of mesopores. It can be observed that the values of specific surface area for FAICS are in the range 0.48-1.22 m^2/g and are lower than for FAI which is 1.72 m^2/g. Similar values of specific surface area and the presence of macropores and mesopores have been recorded by Wan Ngah [24] for chitosan-zeolite composites. It can be observed that for the FAI samples the rise of activation temperature results in the increase of pore size values and decrease of specific surface area. This can be attributed to the fact that the thermally unstable volatile components were liberated at higher temperatures. In the range of 373 K-973 K the specific surface area of fly ash coated chitosan (FAICS) is smaller than that of fly ash (FAI) used for preparation of modified sorbents, whereas pore diameters are higher (except FAICS-773).

The analysis of mineral phases (Table 2) of FAICS and FAI shows the presence of mullite (61.50-70.40%), quartz (26.40-34.80%), hematite (1.90-2.26%), lime (0.00-0.54%), brookite or rutile (0.00-1.80%). For fly ash after activation the contents of mullite have a tendency to rise with the increase of activation temperature. The obtained results showed that modification of FAI, FAI-373,FAI-773 and FAI-1173 by using CS caused increase of mullite content, decrease of quartz and hematite contents as well as elimination of lime and rutile/brookite. The increase of activation temperature and modification by CS have not caused formation of different crystalline phases except rutile in case of FAICS-573. The results by Temuujin and van Riessen [40] obtained by the XRD method also confirm that fly ash contain mullite, quartz and hematite.

To acquire a better understanding of surface chemistry of fly ash during thermal activation the Fourier transform infrared spectra using the attenuated total reflectance technique (FTIR-ATR) of chitosan (CS), fly ash (FAI) and composite (FAICS-373, FAICS-773) were measured. Figs.3a-b show these spectra. The bands at 3436, 1110 and 477 cm^{-1} are assigned to the stretching vibration of the surface hydroxyl, the stretching vibration of Si-O and twisting vibration of Si-O-Si, respectively. The bands for CS can be assigned as follows 3440 cm^{-1}(-OH and -NH_2 stretching vibrations), 2921 cm^{-1} (stretching vibration in -CH and -CH_2), 1652 cm^{-1} (-NH_2 bending vibration) and 1028 cm^{-1} (CO stretching vibration in CONH). Figs.3b shows spectra after Cu(II) ions sorption sorbed of FAICS composite. The band at 1628cm^{-1} of Cu(II) sorbed onto FAICS had a shifting with respect to CS suggesting a chelation complex between the amino groups of CS and Cu(II). Similarly the band at 3600 cm^{-1} has been shifted after the sorption process which indicates that Cu(II) interact with amino and hydroxyl groups of chitosan.

3.2. The effect of temperature activation

It can be observed that for the FAI samples effectiveness of Cu(II) removal decreases with the increase of activation temperature for all studied initial concentrations. The value of q_t for FAI before thermal activation for the investigated metal ions equalled 3.14 mg/g and decreased to 1.12 mg/g for FAI-1173 with the increase of activation temperature. The activation temperature does not affect significantly the sorption capacity of FAICS for Cu(II) because the observed differences of q_t for FAICS samples were not significant. However, the obtained results have clearly shown a significant difference between effectiveness of sorption onto FAI and FAICS, which is higher for the FAICS sorbents.

3.3. The effect of adsorbent dosage

Fig.4a-b presents the comparison of adsorption percentage (*S%*) for Cu(II) onto FAI-373 and FAICS-973 samples. The adsorption percentage for FAI-Cu(II) system was in the range 11.6-65.5%, 19.6-54.4% and 21.9-36.2% for the initial concentration of Cu(II) equal to $1x10^{-3}$, $2x10^{-3}$, $3x10^{-3}$ M, respectively. *S%* for Cu(II) sorption onto FAICS was higher than for FAI. The obtained values were in the range 51.5-98.5%, 63.2-96.6%, 38.0-92.1% for the initial concentration $1x10^{-3}$, $2x10^{-3}$, $3x10^{-3}$ M. It was also revealed that the effect of adsorbent dose on efficiency was significant. Changing the adsorbent dose from 0.05-0.30 g increased the adsorption percentage value for all studied sorbents. It is caused by an increase in the adsorption surface area and the availability of more active adsorption sites [41]. It was found that the maximum adsorption for all investigated heavy metal ions and sorbents was achieved with 0.3 g of adsorbent (data not presented).

3.4. The effect of initial concentration and contact time

The initial concentration and contact time were examined as one of the most important parameters affecting the adsorption process. The results showed in Figs. 5a-e and 6a-d indicate that for all studied sorbents the increase of Cu(II) initial concentration from 1×10^{-3} M to 3×10^{-3} M causes the increase in the adsorbed ions amount (q_t). The values of q_t increase with the phase contact time. For Cu(II) sorption onto all studied sorbents, the process occurs most rapidly for the first few minutes. It can be observed that time to reach equilibrium conditions was in the range from 20 to 30 min. At the equilibrium the maximum percentage of sorption was found to be 98%. On this basis the optimum time for Cu(II) removal was determined to be 60 min. The literature reports that short adsorption time is due to nonporous structure of sorbent and external

adsorption throughout the adsorption process [42]. The above considerations indicate that initial concentrations and contact time played an important role in the Cu(II) ions adsorption onto FAI and FAICS.

3.5. Adsorption kinetics

The experimental data were analyzed according to the linearized form of the pseudo first order (PFO) and the pseudo second order (PSO) equations in order to understand the behaviour of the adsorbents and to investigate the controlling mechanism of the adsorption process. These models were selected due to their good applicability in most cases in comparison with other models [43].The pseudo first order kinetic equation is represented as (Eq.7) [44]:

$$log(q_1 - q_t) = log\, q_1 - \frac{k_1 t}{2.303} \quad (7)$$

where: q_1 and q_t denote the amount of sorption at equilibrium and at time t (mg/g) respectively; k_1 is the rate constant of the pseudo first-order sorption (1/min). Based on the plot of $log\ (q_1-q_t)$ vs. t the kinetic parameters were calculated.

The pseudo second order model is expressed as (Eq.8) [45]:

$$\frac{t}{q_t} = \frac{t}{q_2} + \frac{1}{k_2 q_2^2} \quad (8)$$

where: k_2 is the rate constant of the pseudo second-order sorption (g/mg min). The kinetic parameters were calculated based on the plots of t/q_t vs. t. Furthermore the experimental data were analyzed according to the Weber-Morris kinetic equation, i.e. the intraparticle diffusion model (IPD) [46] given below:

$$q_t = k_i t^{1/2} + C \quad (9)$$

where: k_i is the intraparticle diffusion rate constant (mg/g $min^{0.5}$), C is the intercept which reflects the boundary layer effect.

The kinetic parameters obtained by fitting the kinetic data of Cu(II) adsorption are given in Table 3. It was found that the values of the rate constants of the pseudo first order sorption k_1 are in the range 0.01-0.04. The values of the rate constants k_2 were found to be in the range 0.02-1.62 g/mg min for sorption of Cu(II) ions onto the examined sorbents. It is commonly known that a larger k_2 value suggests that the adsorption systems with low concentrations require a shorter time to achieve a complete sorption. It can be observed that the values of the initial rate constants h were found to increase gradually for Cu(II) sorption onto FAI and FAI 373-1173 as the initial concentration increased from $1x10^{-3}$ to $3x10^{-3}$ M, which confirms that the process is highly concentration dependent. The adsorbate transport from the solution to the surface of the adsorbent occurs in several steps e.g. external diffusion, film diffusion, pore diffusion and adsorption on the pore surface. The process can be regulated by one or more enumerated steps [47].

Dizge et al. [48] report that the adsorption mechanism follows the intraparticular diffusion process (IPD) when the plot of q_t versus $t^{1/2}$ is a straight line with a slope k_i and the intercept C. What is more, the values of the intercept inform about the thickness of a boundary layer, i.e. the larger the intercept is the greater the boundary layer effect. The intraparticle rate k_i of the adsorption of the Cu(II) onto particles of FAI and FAICS is in the range 0.01-0.12 mg/g $min^{0.5}$. It can be also concluded that better determination coefficients (R^2) were obtained with PSO kinetic model (0.99-1.00) compared to the pseudo first order kinetic model. The linear pseudo second order plots (Fig.7a-e) confirm better suitability of pseudo second order kinetic model to describe adsorption kinetics of Cu(II) onto the studied sorbents. Furthermore, q_e and $q_{e,exp}$ in the pseudo second kinetic model are similar.

3.6. Adsorption isotherms studies and adsorption mechanism

Various isotherm equations are used to describe the equilibrium characteristics of adsorption. The Langmuir and Freundlich models are the most common isotherm used to inform how adsorbate molecules distribute between the liquid phase and the solid phase when the adsorption process reaches an equilibrium state [49].These isotherm models are applied in this study for analyzing experimental sorption equilibrium data and obtaining some important information on the surface properties of the adsorbent and its affinity for the investigated metal ions.

The Langmuir isotherm model is based on the assumption that the maximum adsorption occurs when a saturated monolayer of solute molecules is present on the adsorbent surface and the energy of adsorption is constant and there is no migration of absorbate molecules in the surface plane [46, 47]. The model can be presented in the linear form as [50]:

$$\frac{c_e}{q_e} = \frac{1}{q_0 K_L} + \frac{c_e}{q_0} \quad (10)$$

The Freundlich isotherm is an empirical equation based on the heterogeneous surface [51], which is capable of description of multilayer adsorption with interaction between adsorbed molecules [51].

The linear form is expressed by the following equation [52]:

$$log\, q_e = log\, K_F + \frac{1}{n} log\, c_e \quad (11)$$

where: q_0 is the monolayer sorption capacity of chitosan (mg/g) and K_L is a constant related to the free energy sorption (dm^3/mg); K_F (mg/g)(dm^3/mg)$^{1/n}$) and n are the Freundlich constants, characteristic of the system and the indicators of adsorption capacity and reaction energy, respectively.

The dimensionless constant, which characterizes the Langmuir isotherm model, can be the parameter R_L [53] defined by:

$$R_L = \frac{1}{1 + K_L c_0} \tag{12}$$

The adsorption isotherms of Cu(II) onto FAI and FAICS at 293 K, 313 K and 333 K are shown in Figs. 8a-e and 9a-d. It can be observed that the equilibrium data (Table 4) are fitted by the Langmuir isotherm model which is confirmed by the determination coefficient R^2 almost equal to 1.00. The constants K_F and n were calculated from the slope and intercept of the plot between $log\ q_e$ vs. $log\ c_e$. The constant n implies whether the adsorption process is spontaneous [51]. The obtained results show that $1/n$ values are in the range $0.1 < 1/n < 1$ what means that adsorption was favourable [54]. It can be also observed that the parameter R_L, which determines favourable conditions of the Langmuir isotherm (if $R_L < 1$ the process is favourable, if=1 linear and if >1 unfavourable) was lower than 1 for all studied adsorption processes. The exemplary maximum adsorption capacities based on the Langmuir model were equal to 30.58 mg/g for FAI, 34.92 mg/g for FAI-973 and 34.36 mg/g for FAICS-973.

3.7. The effect of temperature

The thermodynamic parameters such as change in the standard free energy (ΔG^o), enthalpy (the heat of adsorption of the adsorbents ΔH^o) and entropy (ΔS^o) for the adsorption process were calculated using (Eq.10) [55]:

$$\Delta G^o = -RT \ln K_c \tag{13}$$

where: R is the gas constant (8.314 J/mol K), T is the temperature (K) and K_C is the equilibrium constant (dm^3/mol) determined by the equation given below:

$$K_c = \frac{c_a}{c_e} \tag{11}$$

where: c_a (mg/dm^3) is the amount of solute adsorbed by the adsorbent at equilibrium and c_e is the equilibrium concentration (mg/dm^3).

The values of thermodynamic parameters are given in Table 5. It was observed that the adsorption amount of Cu(II) increased with the temperature increase from 293 to 333 K. A result of increase in the mobility of the Cu(II) ions with the increasing temperature can be observed. Similar trends were also found for adsorption of heavy metal ions onto fly ash [56].

For all investigated systems $\ln K_c$ was plotted against $1/T$ and the plots were found to be linear. These plots were used to determine ΔH^o and ΔS^o from the intercept and slope respectively. The calculated $\Delta H°$ were positive values which indicates that adsorption processes were endothermic. The magnitude of the ΔH^o value for physical adsorptions is in the range of 2.1–20.9 while for chemical adsorptions in the range 80–200 kJ/mol [57]. It can be observed that for all studied cases ΔH^o values were low which implies physical adsorption of Cu(II) ions. The negative values of ΔS^o indicate decrease randomness at the solid-solution interface during the fixation of adsorbates on the active sites of the composite FAICS [58]. The values of ΔG^o were also negative which indicates that the process was thermodynamically spontaneous, favourable and feasible. The process was controlled by physical adsorption because the ΔG^o values were higher than −20 kJ/mol [59].

4. Conclusions

This paper has clearly shown a significant difference between effectiveness of sorption onto FAI and FAICS, which is higher for the FAICS sorbents. It means that efficiency of Cu(II) removal from aqueous solution is dependent on the various factors in which the type of sorbent is the most important. The efficiency of Cu(II) removal from aqueous solution using both the FAI and FAICS samples also depends on the amount of adsorbent, phase contact time and initial concentrations. The increasing sorption efficiency with the rise of listed experimental parameters was observed. The adsorption equilibrium was reached after 20-30 min. However, the temperature activation does not have so great influence on sorption capacity of the studied sorbents for Cu(II) as modification by using chitosan.

The obtained results indicate that Cu(II) sorption onto FAI and FAICS can be well described by the pseudo second order model, which is confirmed by better determination coefficients (R^2) with the pseudo second order kinetic model (almost equal to 1.00) compared to the pseudo first order kinetic model. The maximum adsorption capacity based on the Langmuir model were equal to 30.58 mg/g for FAI, 34.92 mg/g for FAI-973 and 34.36 mg/g for FAICS-973.The adsorption studies showed that the Langmuir isotherm model fitted the equilibrium data for Cu(II) both onto FAI and FAICS better than the Freundlich isotherm model which is confirmed by the determination coefficient R^2 almost equal to 1.0. Based on the thermodynamic data, it can be concluded that the process is spontaneous, favourable and feasible as well

as endothermic in nature as evidenced by the negative values of ΔG^o and positive ΔH°. The research indicates an increase in the adsorption capacity with the increasing temperature.

The proposed method of enhancing the efficiency of heavy metal ions removal from aqueous solution and what is important by using inexpensive sorbent can be readily applied in practice. This solution has great potential for applications due to its abundance and ready availability. Further study of the subject is still required in order to find the best content of chitosan to achieve both fast kinetics and high adsorption capacity as well as to find definite answer if it is necessary to activate fly ash before modification by using chitosan or what kind of activation method will be the most effective in this case.

References:

[1] Coal Facts 2014, http://www.worldcoal.org/resources/coal-statistics/ (2015) Accessed 7 March 2015.

[2] Production and Utilisation of CCPs in 2010 in Europe, http://www.ecoba.com/evjm,media/ccps/ECO-STAT_2010.pdf (2015) Accessed 7 March 2015.

[3] http://www2.epa.gov/coalash/coal-ash-reuse (2015) Accessed 7 March 2015.

[4] Van Jaarsveld, J.S.G., Van Deventer, J.S.J, Lukey, G.C.: The characterization of source materials in fly ash-based geopolymers. Mater. Lett. 57, 1272–1280 (2003)

[5] Kurdowski, W.: Chemia cementu. PWN, Warszawa (1990)

[6] Temuujin, J., van Riessen, A., Williams, R.: Influence of calcium compounds on the mechanical properties of fly ash geopolymer pastes. J. Hazard. Mater. 167, 82–88 (2009)

[7] Sztekler, D., Majchrzak – Kucęba, I, Nowak, W.: Analysis of the chemical composition of coal fly ash for synthesis zeolite Na–A http://wis.pol.lublin.pl/kongres3/tom1/34.pdf (2015) Accessed 7 March 2015

[8] American Society for Testing and Materials (ASTM), ASTM C618–12a, Standard specification for coal fly ash and raw or calcined natural pozzolan for use in concrete, Annual book of ASTM standards. Philadelphia, Pennsylvania (1994)

[9] Xu, A.: Fly ash in concrete. In: Chandra, S. (ed.) Waste Materials Used in Concrete Manufacturing, pp. 142–183. William Andrew Pub., Norwich (1997)

[10] Koukouzas, N. , Hämäläinen, J., Papanikolaou, D., Tourunen, A. , Jäntti, T.: Mineralogical and elemental composition of fly ash from pilot scale fluidised bed combustion of lignite, bituminous coal, wood chips and their blends. Fuel 86, 2186–2193 (2007)

[11] Dimter, S., Rukavina, T., Barišić, I.: Alternative, environmentally acceptable materials in road constructions. In: Gaurina-Medjimurec, N. (ed.) Handbook of research on advancements in environmental engineering, pp.318-348. Engineering Science Reference IGI, USA (2015)

[12] Muñoz, M.I., Aller, A.J.: Chemical modification of coal fly ash for the retention of low levels of lead from aqueous solutions. Fuel 102, 135–144 (2012)

[13] Derkowski, A., Franus, W., Beran, E., Czimerova, A.,: Properties and potential applications of zeolitic materials produced from fly ash using simple method of synthesis. Powder Technol., 166(1), 47–54 (2006)

[14] Katara, S., Kabra, S., Sharma, A., Hada, R., Rani, A.: Surface Modification of Fly Ash by Thermal Activation: A DR/FTIR Study. Internat. Res. J. Pure App. Chem. 3(4), 299–307 (2013)

[15] Mishra, S.B., Langwenya, S.P., Mamba, B.B., Balakrishnan, M.: Study on surface morphology and physicochemical properties of raw and activated South African coal and coal fly ash. Phys. Chem. Earth 35, 811–814 (2010)

[16] Everson, R.C., Neomagus, H.W.J.P., Kaitano, R., Falan, R., van Alphen, C., Properties of high ash char particles derived from inertinite-rich coal: 1.Chemical, structural and petrographic characteristics. Fuel 87 3082–3290 (2008)

[17] Lu, P., Xu, S., Chu, X.: Pyrolysis property of pulverized coal in an entrained flow reactor during coal reburning. Chem. Eng. Process. 48, 333–338 (2008)

[18] Temuujin, J., van Riessen, A.: Effect of fly ash preliminary calcination on the properties of geopolymer, J. Hazard. Mater. 164, 634–639 (2009).

[19] Wen, Y., Tang, Z., Chen, Y., Gub, Y.: Adsorption of Cr(VI) from aqueous solutions using chitosan-coated fly ash composite as biosorbent. Chem. Eng. J. 175, 110–116 (2011)

[20] Xie, J., Li, Ch., Chi, L., Wu, D., Chitosan modified zeolite as a versatile adsorbent for the removal of different pollutants from water. Fuel 103, 480–485 (2013)

[21] Kamari, A., Ngah, W.S.W., Chong, M.Y., Cheah, M.L.: Sorption of acid dyes onto GLA and H_2SO_4 cross-linked chitosan beads. Desalination 249, 1180–1189 (2009).

[22] Guibal, E.: Interactions of metal ions with chitosan-based sorbents: a review. Sep. Purif. Technol. 38, 43–74 (2004)

[23] Kołodyńska, D.: Chitosan as an effective low-cost sorbent of heavy metal complexes with the polyaspartic acid. Chem. Eng. J. 173, 520–529 (2011)

[24] Wan Ngah, W.S., Teong, L.C., Hanafiah, M.A.K.M.: Adsorption of dyes and heavy metal ions by chitosan composites: A review. Carbohydr. Polym. 83, 1446–1456 (2011)

[25] Eikenes, M., Fongen, M., Roed, L., Stenstrøm, Y.: Determination of chitosan in wood and water samples by acidic hydrolysis and liquid chromatography with online fluorescence derivatization. Carbohydr. Polym. 61, 29–38 (2005)
[26] Kasaai, M. R.: Determination of the degree of N-acetylation for chitin and chitosan by various NMR spectroscopy techniques: A review. Carbohydr. Polym. 79, 801–810 (2010)
[27] Berth, G., Dautzenberg, H., Peter. M.G.: Physico-chemical characterization of chitosans varying in degree of acetylation. Carbohydr. Polym. 36, 205–216 (1998)
[28] Kurita, K.: Chitin and chitosan: Functional biopolymers from marine crustaceans. Marine Biotechnology, 8 (2006) 203–226.
[29] Rinaudo, M.: Chitin and chitosan: Properties and applications. Prog. Polym. Sci. 31 603–632 (2006)
[30] Dash, M., Chiellini, F., Ottenbrite, R.M., Chiellini, E.: Chitosan–A versatile semi-synthetic polymer in biomedical applications. Prog. Polym. Sci. 36, 981–1014 (2011)
[31] Davidovich-Pinhas, M., Danin-Poleg, Y., Kashi, Y., Bianco-Peled, H.: Modified chitosan: A step toward improving the properties of antibacterial food packages. Food Packaging and Shelf Life 1(2) 160–169 (2014).
[32] Ramos V.M., Rodrıguez N.M., Rodrıguez M.S., Heras A., Agulló E.: Modified chitosan carrying phosphonic and alkyl groups. Carbohydr. Polym. 51, 425–429 (2003)
[33] Zhang, W., Xiao, H., Qian, L.: Beeswax– chitosan emulsion coated paper with enhanced water vapor barrier efficiency. Appl. Surf. Sci. 300, 80–85 (2014)
[34] Kananont, N., Pichyangkura, R., Chanprame, S., Chadchawan, S., Limpanavech, P.: Chitosan specificity for the *in vitro* seed germination of two *Dendrobium*orchids (Asparagales: Orchidaceae). Sci. Hortic. 124(2), 239–247 (2010)
[35] Lopez-Ramon, M.V., Stoeckli, F., Moreno-Castilla, C., Carraso-Marin, F.: On the characterization of acidic and basic surface sites on carbons by various techniques. Carbon 37, 1215–1221 (1999)
[36] Adamczuk A., Kołodyńska, D.: Removal of chromium, copper, zinc and arsenic from aqueous solutions onto fly ash coated by chitosan. equilibrium, thermodynamic and kinetic studies. Chem. Eng. J. doi:10.1016/j.cej.2015.03.088
[37] Ricou-Hoeffer, P., Lecuyer, I., Le Cloirec, P.: Experimental design methodology applied to adsorption of metallic ions onto fly ash. Water Res. 35(4), 965–976 (2001)
[38] DSun, D., Zhang, X., Wu, Y., Liu, X.: Adsorption of anionic dyes from aqueous solution on fly ash. J. Hazard. Mater. 181, 335–342 (2010)
[39] Rouquerol J., Avnir D., Fairbridge C.W., Recommendations for the characterization of porous solids. Pure App. Chem. 66, 1739–1758 (1994).
[40] Temuujin, J. , van Riessen A.: Effect of fly ash preliminary calcination on the properties of geopolymer. J. Hazard. Mater. 164, 634–639 (2009)
[41] Kara, S., Aydiner, C., Demirbas, E., Kobya, M., Dizge, N.: Modeling the effects of adsorbent dose and particle size on the adsorption of reactive textile dyes by fly ash. Desalination 212, 282–293(2007)
[42] Nassar, N.N., Ringsred, A. Rapid adsorption of methylene blue from aqueous solutions by goethite nanoadsorbents. Environ. Eng. Sci. 29(8), 790–797 (2012)
[43] Argun, M.E., Dursun, S. A new approach to modification of natural adsorbent for heavy metal adsorption. Bioresource Technol. 99, 2516–2527 (2008)
[44] Lagergren, S. Zur theorie der sogenannten adsorption gelosterstoffe. Kungliga Svenska Vetenskapsakademiens Handlingar 24, 1–39 (1898).
[45] Ho, Y.S., McKay, G. Sorption of dye from aqueous solution by peat. Chem. Eng. J., 70 115–124 (1998).
[46] Weber, W.J., Morris, J.C. Kinetics of adsorption on carbon from solution. J. Sanit. Eng. Div. Am. Soc. Civil Eng., 89, 31–59 (1963)
[47] Demirbas E., Nas M.Z. Batch kinetic and equilibrium studies of adsorption of Reactive Blue 21 by fly ash and sepiolite. Desalination 243, 8–21 (2009)
[48] Dizge, N., Aydiner, C., Demirbas, E., Kobya, M., Kara, S. Adsorption of reactive dyes from aqueous solutions by fly ash: Kinetic and equilibrium studies. J Hazard Mater 150, 737–746 (2008)
[49] Hasan, M. Adsorption of reactive dye onto cross-linked chitosan/oil palm ash composite beads. Chem Eng J 136, 164–172 (2008)
[50] I. Langmuir, The constitution and fundamental properties of solids and liquids, Journal of American Chemical Society, 38 (1916) 2221–2295.
[51] Li, H., Bi, S., Liu, L., Dong, W., Carbohyd, X. Separation and accumulation of Cu(II), Zn(II) and Cr(VI) from aqueous solution by magnetic chitosan modified with diethylenetriamine. Desalination 278, 397–404 (2011)
[52] Freundlich, H.F.M. Über die adsorption in lösungen. Z. Phys. Chem. 57, 385–470 (1906).
[53] Hall, K.R., Eagleton, L.C., Acrivos, A., Vermeulen, T. Pore- and solid-diffusion kinetics in fixed-bed adsorption under constant pattern conditions. Ind. Eng. Chem. Fundam. 5, 212–223 (1966)
[54] Li, K.Q., Wang, X.H. Adsorptive removal of Pb(II) by activated carbon prepared from Spartina alterniflora: equilibrium, kinetics and thermodynamics. Bioresource Technol. 100, 2810–2815 (2009)

[55] Albadarin, A.B., Mangwandi, Ch., Al-Muhtaseb, A.H., Walker, G.W., Allen, S.J., Ahmad, M.N.M. Kinetic and thermodynamics of chromium ions adsorption onto low-cost dolomite adsorbent. Chem. Eng. J. 179, 193–202 (2012)
[56] Tofan, L., Paduraru, C., Bilba, D., Rotariu, M.: Thermal power plants ash as sorbent for the removal of Cu(II) and Zn(II) ions from wastewaters. J Hazard. Mater. 156, 1–8 (2008)
[57] Wang S., Wu, H.: Environmental-benign utilisation of fly ash as low-cost adsorbents. J. Hazard. Mater. 136, 482–501 (2006)
[58] Zimmermann, A.C., Mecabô, A., Fagundes, T., Rodrigues, C.A.: Adsorption of Cr(VI) using Fe-crosslinked chitosan complex (Ch-Fe), J. Hazard. Mater. 179, 192–196 (2010).
[59] Ali, S.A., El-Shareef, A.M., Al-Ghamdi, R.F., Saeeda, M.T.: The isoxazolidines: the effects of steric factor and hydrophobic chain length on the corrosion inhibition of mild steel in acidic medium. Corr. Sci. 47, 2659–2678 (2005).

(a)

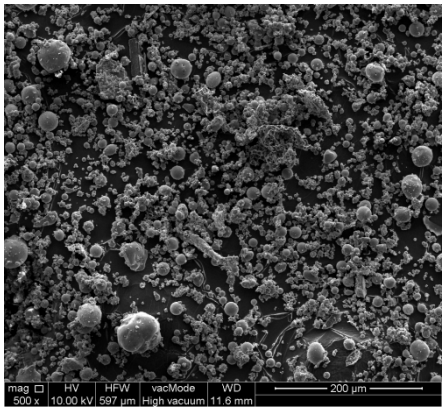

(b)

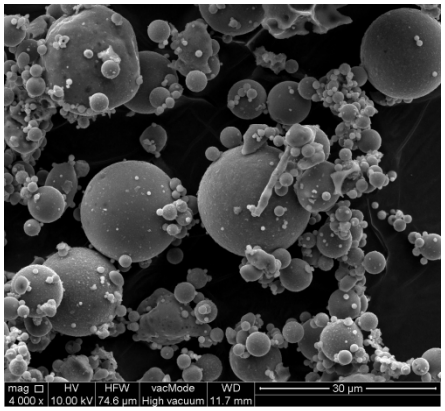

(c)

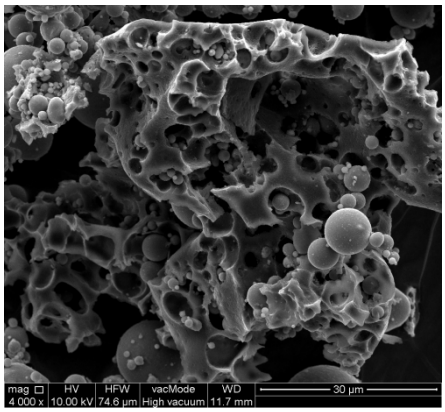

(d)

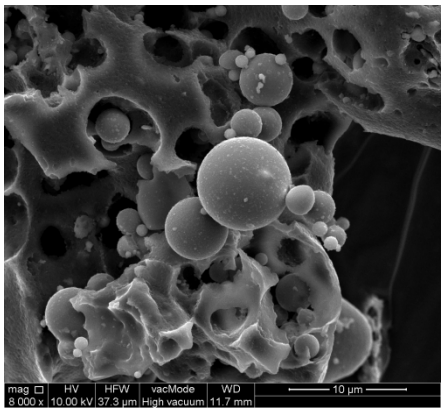

Figs.1a-d. SEM images of: a) FAI-373, b) FAI-1173 and c) FAICS-373, d) FAICS-1173.

(a)

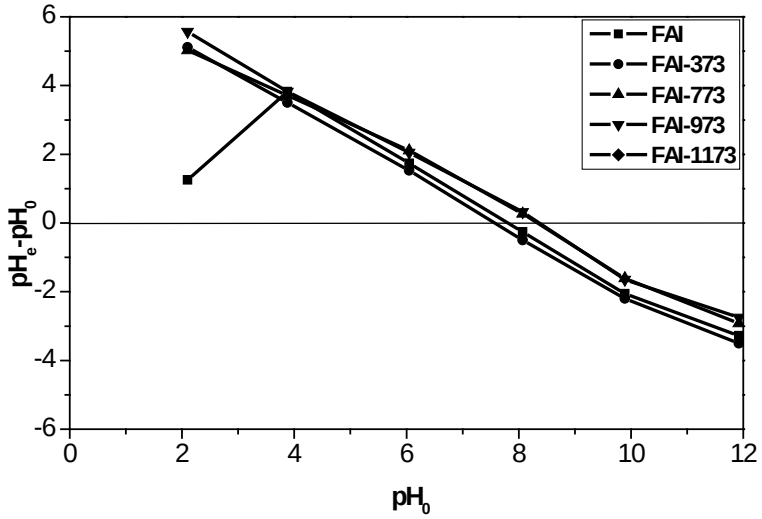

(b)

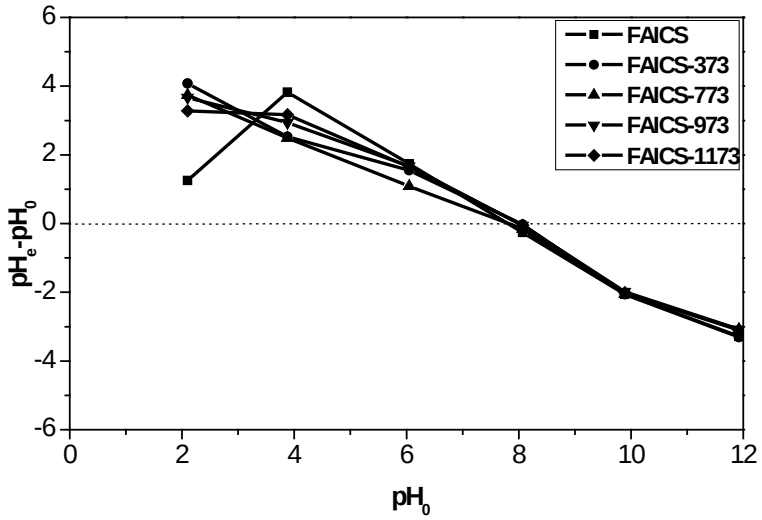

Figs.2a-b. Determination of pH_{pzc} of: a) FAI, FAI-373, FAI-773, FAI-973, FAI-1173 and b) CS, FAICS-373, FAICS-773, FAICS-973, FAICS-1173.

(a)

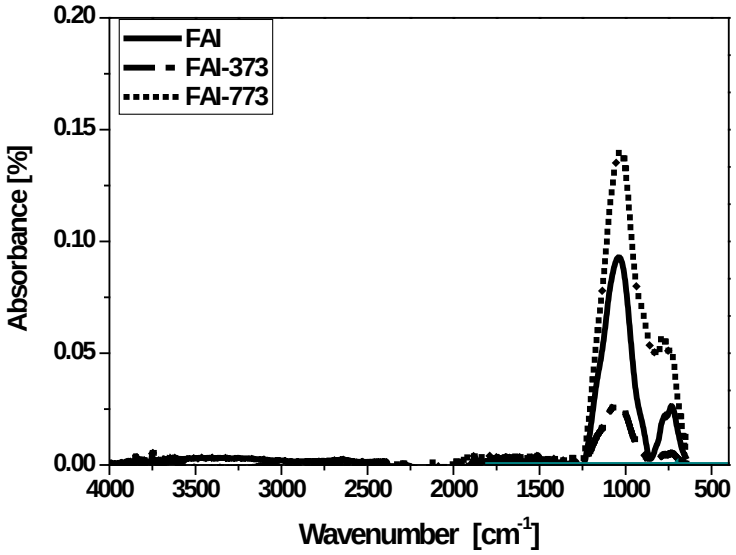

(b)

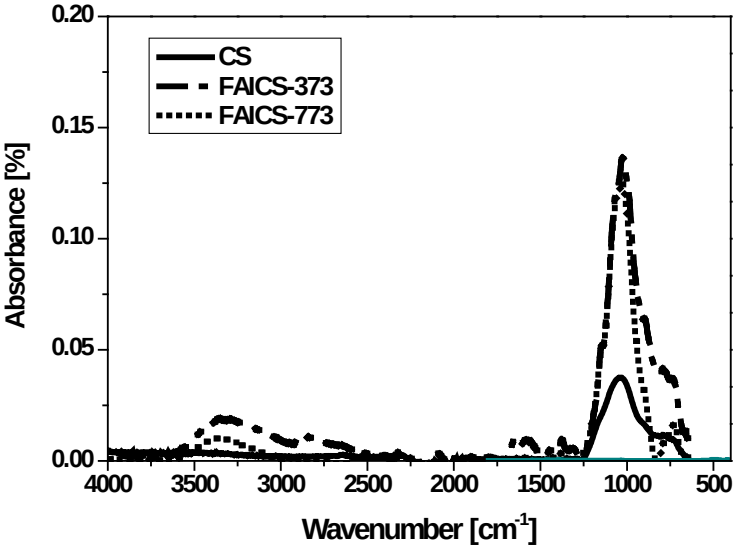

Fig.3a-b. FT-IR spectra of: a) FAI, FAI-373, FAI-773 and b) CS, FAICS-373, FAICS-773.

(a)

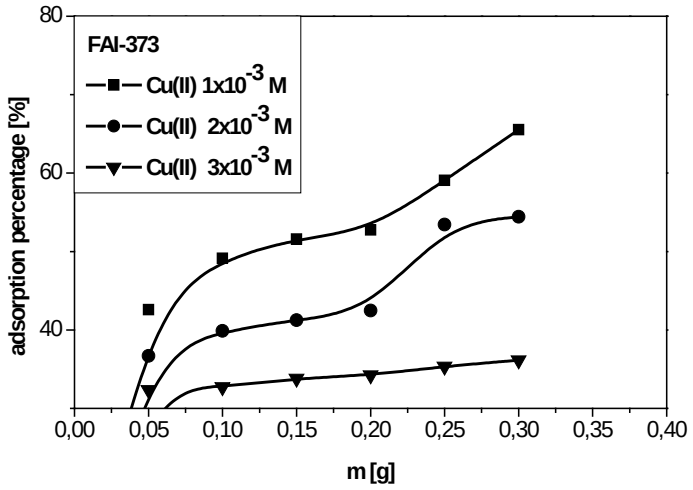

(b)

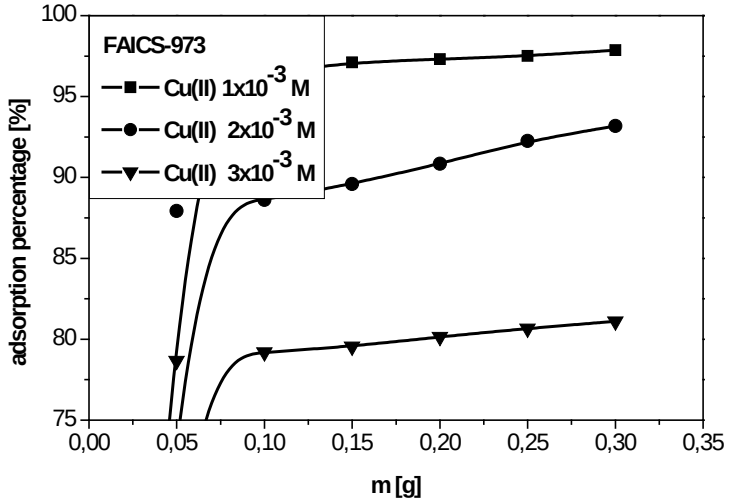

Fig.4a-b. The adsorption percentage for sorption of Cu(II) onto a) FAI-373 and b) FAICS-973 samples according to adsorbent dosage.

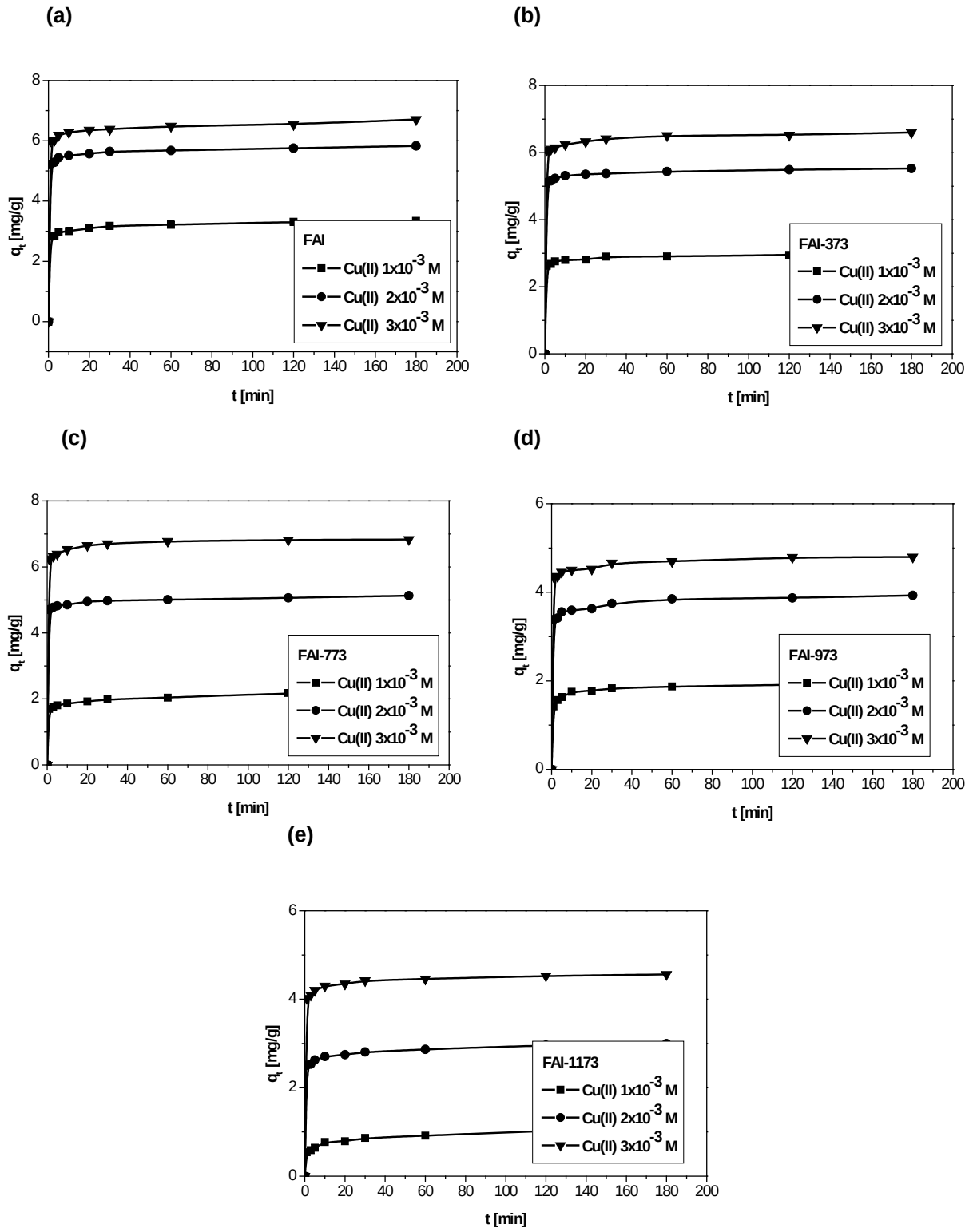

Fig.5a-e. Effect of contact time for the adsorption of Cu(II): a) FAI b) FAI-373, c) FAI-773, d) FAI-973, e) FAI-1173 (initial concentration $1 \div 3 \times 10^{-3}$ M, temperature 293 K, contact time 180 min, adsorbent dose 0.2 g, shaking speed 180 rpm).

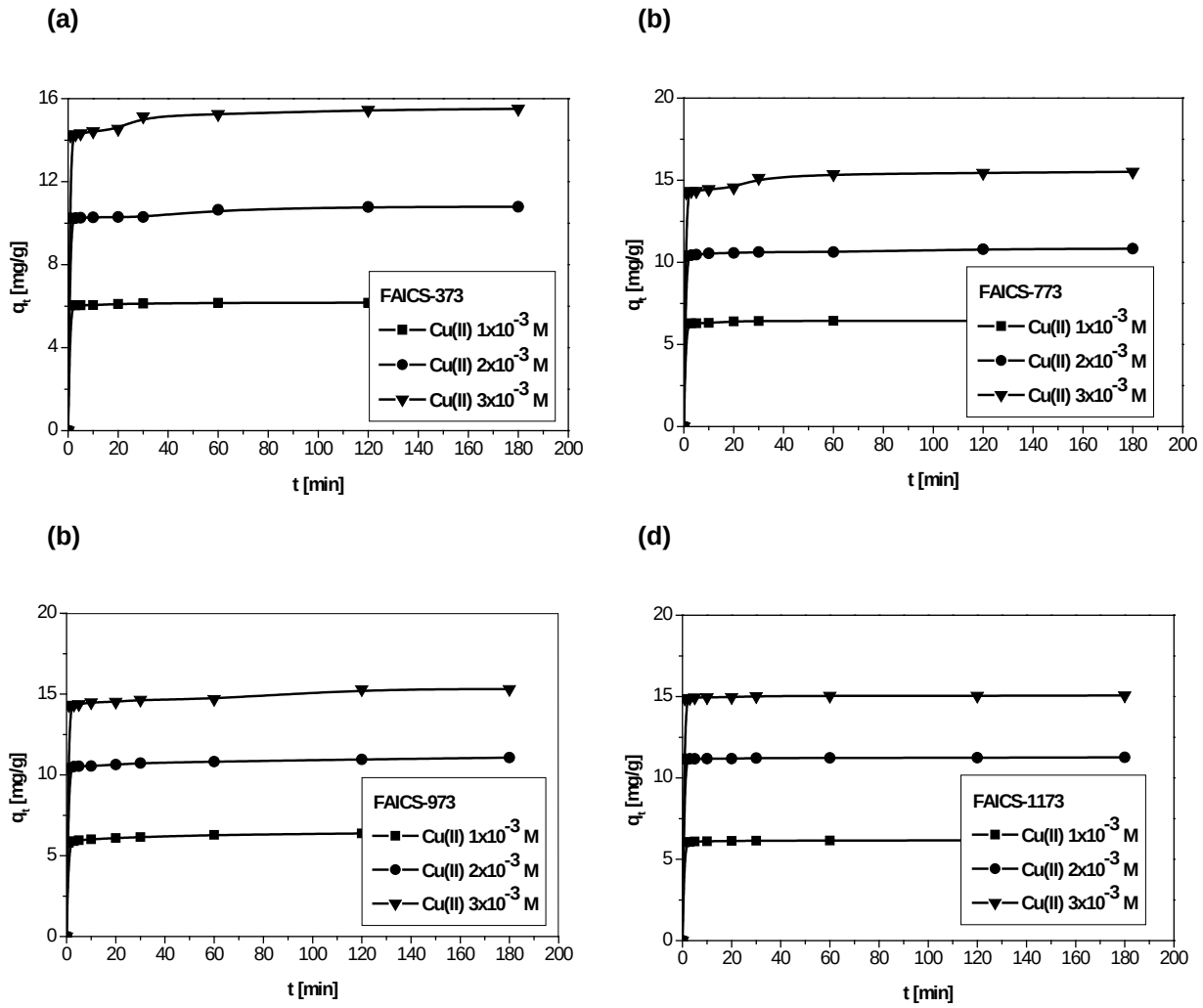

Fig.6a-d. Effect of contact time for the adsorption of Cu(II): a) FAICS-373, b) FAICS-773, c) FAICS-973, d) FAICS-1173 (initial concentration 1÷3x10^{-3} M, temperature 293 K, contact time 180 min, adsorbent dose 0.2 g, shaking speed 180 rpm).

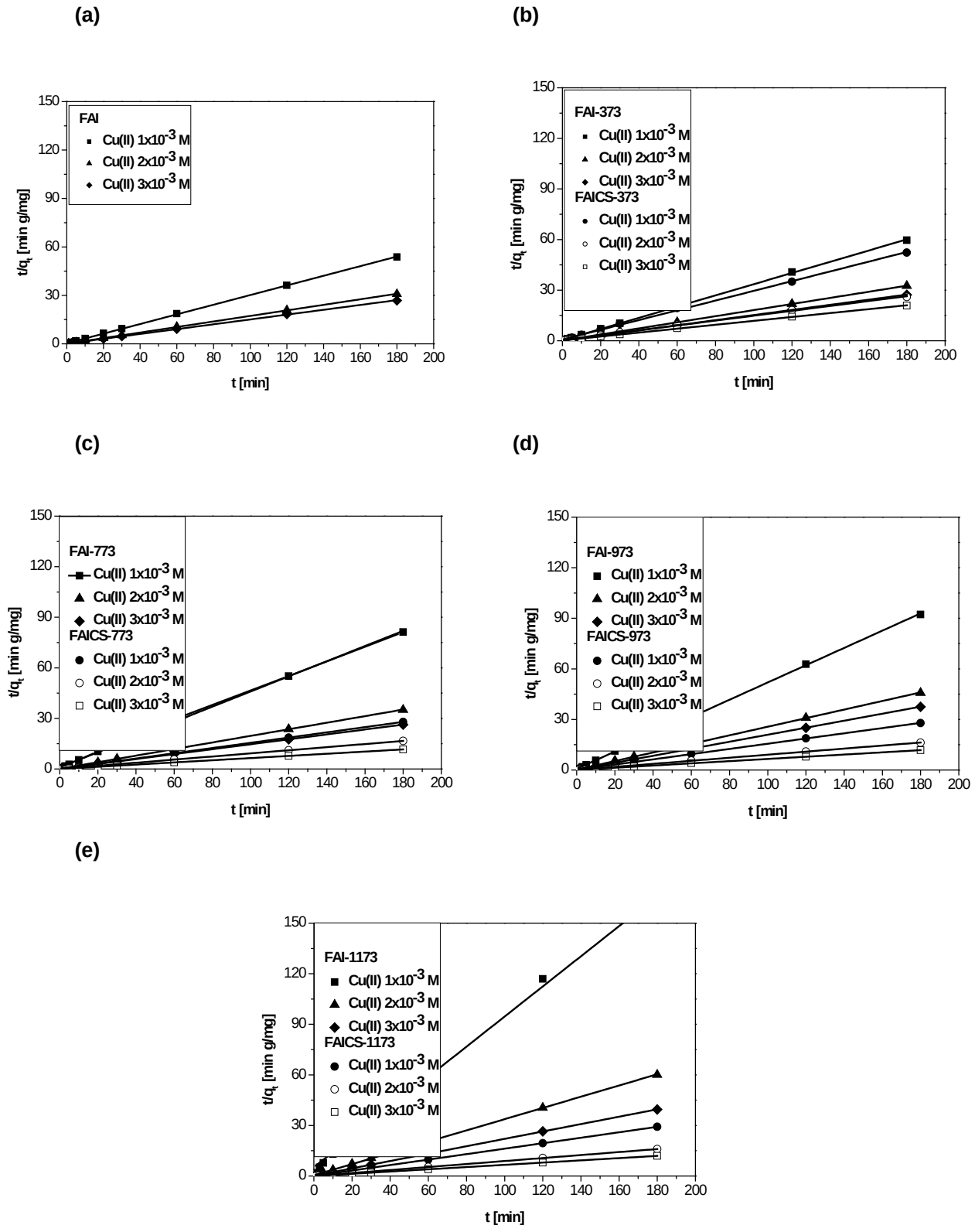

Fig.7a-e. The pseudo second order plots of Cu(II) onto a) FAI, b) FAI-373 and FAICS-373, c) FAI-773 and FAICS-773, d) FAI-973 and FAICS-973 e) FAI-1173 and FAICS-1173 (initial concentration $1 \div 3 \times 10^{-3}$ M, temperature 293 K, contact time 180 min., adsorbent dosage 0.2 g, shaking speed 180 rpm).

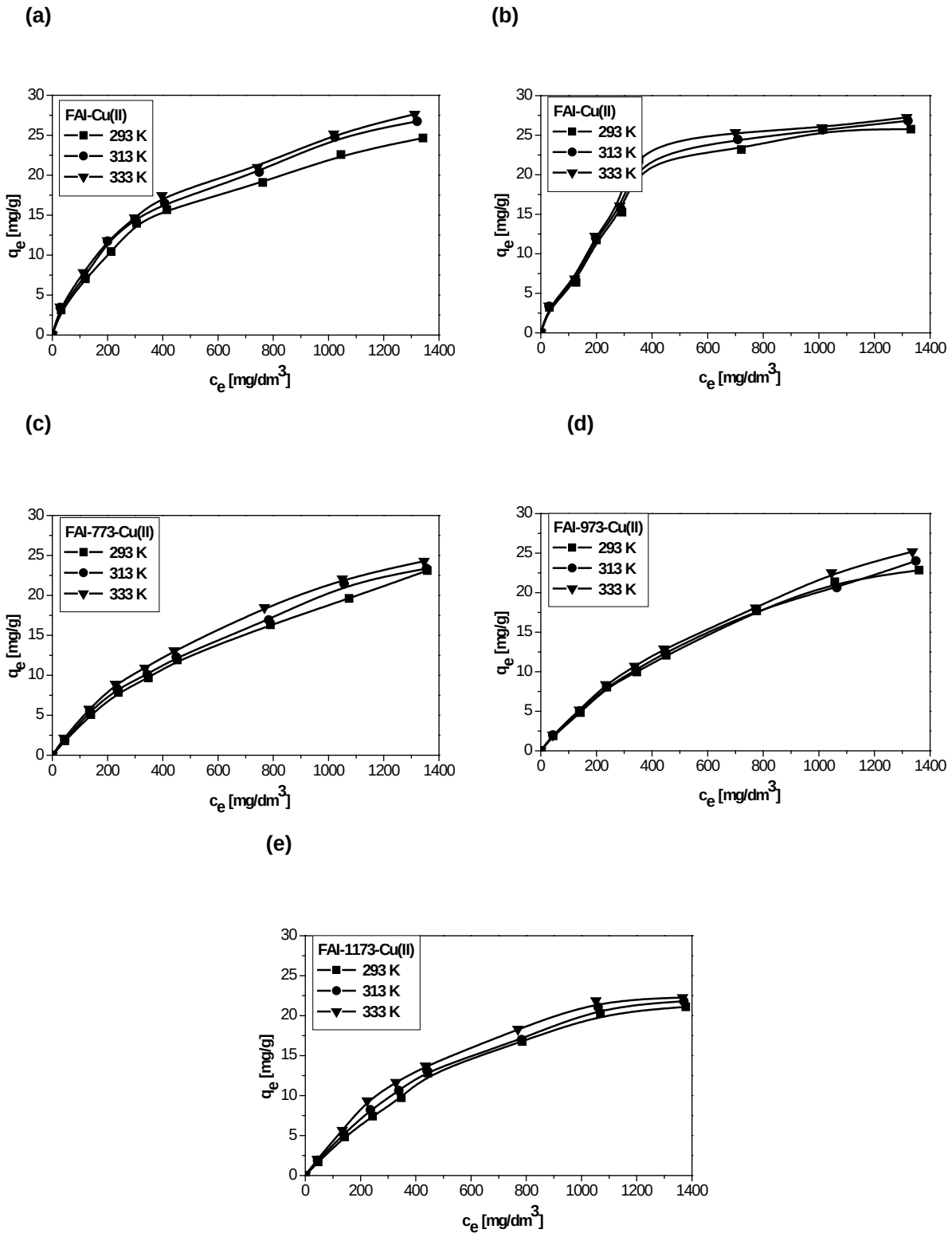

Figs.8a-e. The adsorption isotherms of Cu(II) onto: a) FAI, b) FAI-373, c) FAI-773, d) FAI-973, e) FAI-1173 at temperature 293 K, 313 K and 333 K.

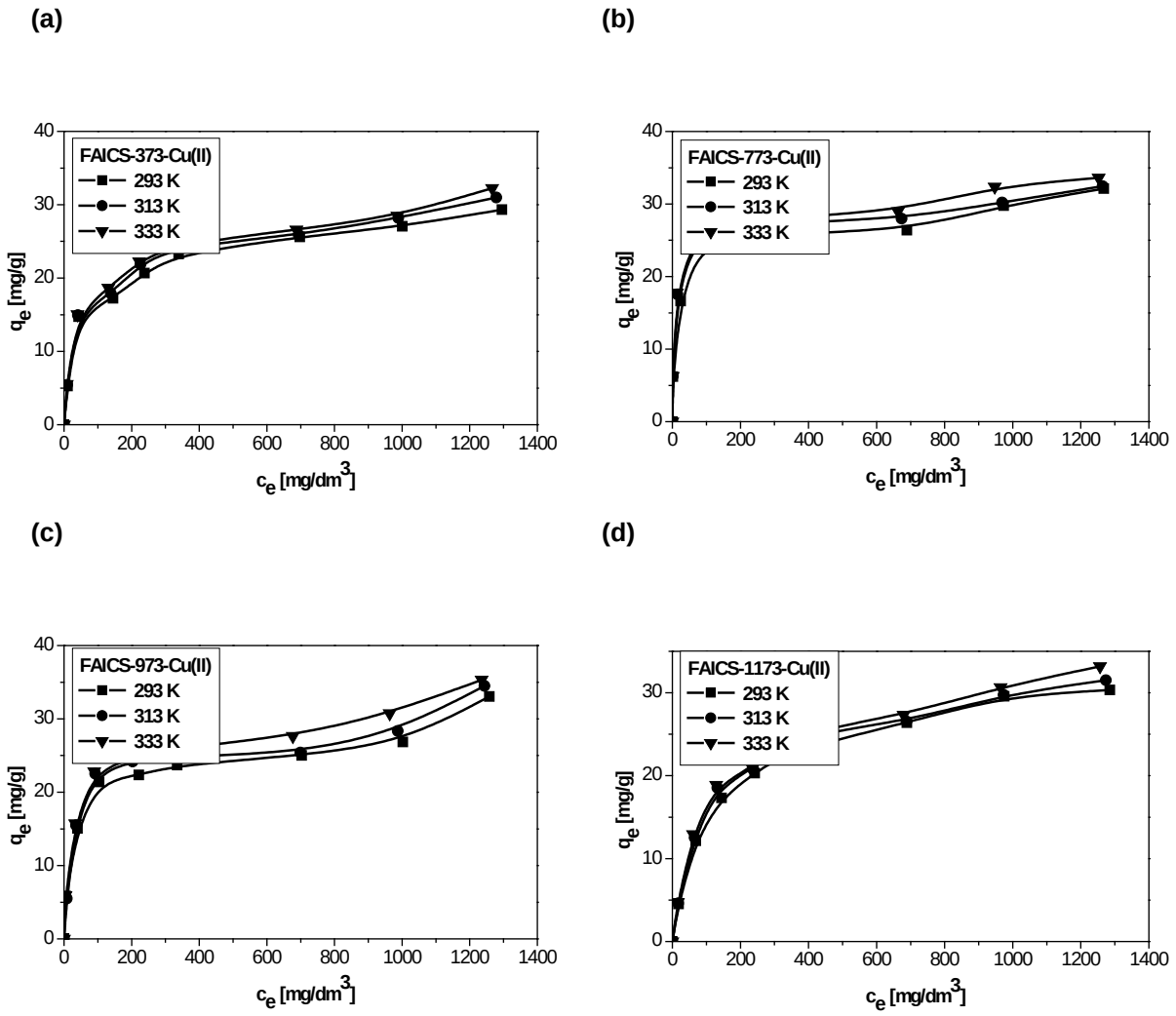

Figs.9a-d. The adsorption isotherms of Cu(II) onto: a) FAICS-373, b) FAICS-773, c) FAICS-973, d) FAICS-1173 at temperature 293 K, 313 K and 333 K.

Table 1. The values of the pore size and the surface area for FAI after thermal activation and modification by using chitosan.

Adsorbent	Specific surface area (m^2/g)	Average pore diameter (nm)
FAI	1.72	9.4
FAI-373	1.22	20.4
FAI-773	1.37	31.2
FAI-973	0.72	32.4
FAI-1173	0.36	31.7
FAICS-373	0.83	32.2
FAICS-773	0.81	26.7
FAICS-973	0.63	36.9
FAICS-1173	0.48	34.35

Table 2. The results of analysis of the states of mineral phases.

Adsorbent	Mullite $Al_6Si_2O_{13}$ (%wt)	Hematite Fe_2O_3 (%wt)	Lime CaO (%wt)	Brookite/Rutile TiO_2 (%wt)	Quartz SiO_2 (%wt)
FAI	75.80	3.50	0.00	1.80	20.00
FAI-373	61.50	1.90	0.38	1.50	34.80
FAI-773	62.00	1.60	0.46	1.60	34.20
FAI-973	67.00	2.26	0.20	1.60	29.40
FAI-1173	68.00	2.20	0.00	1.80	29.40
FAICS-373	67.00	1.50	0.00	0.00	31.70
FAICS-773	65.90	1.50	0.00	0.00	31.50
FAICS-973	66.10	2.30	0.00	0.00	31.60
FAICS-1173	70.40	2.00	0.00	0.00	26.40

Table 3. Kinetic parameters for the adsorption of Cu(II) onto FAI, FAI-373, FAI-773, FAI-973, FAI-1173, FAICS-373, FAICS-773, FAICS-973, FAICS-1173.

PFO				PSO				IPD	
C_0 (M)	q_1 (mg/g)	k_1 (g/mgmin)	R^2	q_2 (mg/g)	k_2 (g/mgmin)	h	R^2	k_i (mg/g $min^{0.5}$)	R^2
FAI									
$1x10^{-3}$	0.44	0.02	0.96	3.35	0.27	3.00	1.00	0.04	0.89
$2x10^{-3}$	0.44	0.02	0.87	5.82	0.26	8.71	1.00	0.04	0.85
$3x10^{-3}$	0.54	0.01	0.83	6.68	0.18	7.96	1.00	0.05	0.90
FAI-373									
$1x10^{-3}$	0.29	0.01	0.81	3.01	0.35	3.19	1.00	0.03	0.87
$2x10^{-3}$	0.32	0.02	0.95	5.53	0.37	11.40	1.00	0.03	0.88
$3x10^{-3}$	0.43	0.02	0.86	6.60	0.28	11.98	1.00	0.04	0.90
FAI-773									
$1x10^{-3}$	0.48	0.02	0.98	2.22	0.21	1.02	1.00	0.04	0.96
$2x10^{-3}$	0.32	0.02	0.88	5.12	0.34	8.83	1.00	0.03	0.90
$3x10^{-3}$	0.45	0.03	0.97	6.85	0.36	16.86	1.00	0.05	0.80
FAI-973									
$1x10^{-3}$	0.32	0.02	0.85	1.95	0.38	1.43	1.00	0.04	0.76
$2x10^{-3}$	0.43	0.02	0.89	3.93	0.28	4.26	1.00	0.04	0.88
$3x10^{-3}$	0.45	0.03	0.98	4.81	0.31	7.14	1.00	0.04	0.90
FAI-1173									
$1x10^{-3}$	0.48	0.01	0.94	1.12	0.15	0.19	1.00	0.04	0.94
$2x10^{-3}$	0.42	0.02	0.98	3.00	0.27	2.41	1.00	0.04	0.91
$3x10^{-3}$	0.39	0.02	0.93	4.57	0.32	6.72	1.00	0.04	0.83
FAICS-373									
$1x10^{-3}$	0.16	0.01	0.80	6.20	0.63	24.33	1.00	0.02	0.93
$2x10^{-3}$	0.83	0.04	0.93	10.81	0.16	18.38	1.00	0.05	0.91
$3x10^{-3}$	1.30	0.03	0.97	15.55	0.10	23.59	1.00	0.12	0.89
FAICS-773									
$1x10^{-3}$	0.14	0.04	0.94	6.45	1.29	53.48	1.00	0.02	0.76
$2x10^{-3}$	0.42	0.02	0.93	10.83	0.25	29.67	1.00	0.04	0.95
$3x10^{-3}$	1.22	0.03	0.93	15.55	0.10	25.25	1.00	0.12	0.88
FAICS-973									
$1x10^{-3}$	0.56	0.02	0.97	6.46	0.19	7.73	1.00	0.05	0.96
$2x10^{-3}$	0.58	0.01	0.98	11.06	0.17	20.20	1.00	0.05	0.98
$3x10^{-3}$	1.33	0.03	0.86	15.34	0.08	19.31	1.00	0.09	0.95
FAICS-1173									
$1x10^{-3}$	0.09	0.02	0.90	6.17	1.62	61.73	1.00	0.01	0.77
$2x10^{-3}$	0.09	0.01	0.90	11.26	1.11	140.85	1.00	0.01	0.96
$3x10^{-3}$	0.14	0.02	0.79	15.08	0.90	204.08	1.00	0.02	0.83

Table 4. Langmuir and Freundlich parameters for adsorption of Cu(II) onto FAI, FAI-373, FAI-773, FAI-973, FAI-1173, FAICS-373, FAICS-773, FAICS-973, FAICS-1173.

Adsorbent	T (K)	Langmuir model				Freundlich model		
		q_0 (mg/g)	K_L (dm^3/mg)	R_L (-)	R^2	K_F (mg/g)	1/n	R^2
FAI	293	30.58	$2.66x10^{-3}$	0.19	0.99	0.51	0.55	0.98
	313	33.32	$2.68x10^{-3}$	0.19	0.98	0.59	0.54	0.99
	333	33.67	$2.83x10^{-3}$	0.18	0.98	0.64	0.54	0.99
FAI-373	293	33.78	$2.83x10^{-3}$	0.18	0.96	0.46	0.59	0.92
	313	34.48	$2.95x10^{-3}$	0.18	0.96	0.50	0.58	0.93
	333	34.72	$3.12x10^{-3}$	0.17	0.96	0.53	0.58	0.91
FAI-773	293	37.45	$1.07x10^{-3}$	0.37	0.98	0.13	0.73	0.99
	313	38.17	$1.13x10^{-3}$	0.36	0.98	0.14	0.73	0.98
	333	37.31	$1.33x10^{-3}$	0.32	0.99	0.18	0.69	0.99
FAI-973	293	38.76	$1.05x10^{-3}$	0.37	0.99	0.13	0.74	0.99
	313	40.16	$1.06x10^{-3}$	0.37	0.99	0.14	0.73	0.99
	333	42.92	$1.02x10^{-3}$	0.38	0.99	0.14	0.74	0.99
FAI-1173	293	36.23	$1.10x10^{-3}$	0.37	0.99	0.11	0.75	0.98
	313	34.72	$1.30x10^{-3}$	0.33	0.99	0.15	0.71	0.98
	333	33.44	$1.60x10^{-3}$	0.28	0.99	0.18	0.69	0.97
FAICS-373	293	30.12	$1.17x10^{-2}$	0.05	0.99	3.27	0.32	0.90
	313	31.45	$1.18x10^{-2}$	0.05	0.99	3.49	0.32	0.91
	333	32.26	$1.20x10^{-2}$	0.05	0.99	3.67	0.31	0.92
FAICS-773	293	31.45	$2.40x10^{-2}$	0.03	0.99	6.92	0.23	0.91
	313	31.85	$3.29x10^{-2}$	0.02	1.00	7.78	0.22	0.87
	333	33.33	$3.21x10^{-2}$	0.02	1.00	8.33	0.21	0.90
FAICS-973	293	31.25	$1.37x10^{-2}$	0.04	0.97	4.67	0.27	0.91
	313	32.68	$1.36x10^{-2}$	0.04	0.97	4.16	0.30	0.84
	333	34.36	$1.50x10^{-2}$	0.04	0.98	4.93	0.28	0.91
FAICS-1173	293	33.22	$7.31x10^{-3}$	0.08	1.00	1.74	0.42	0.93
	313	33.67	$8.00x10^{-3}$	0.07	1.00	1.92	0.41	0.91
	333	35.21	$7.70x10^{-3}$	0.08	0.99	2.02	0.41	0.92

Table 5. Thermodynamic data for adsorption of Cu(II) onto FAI, FAI-373, FAI-773, FAI-973, FAI-1173, FAICS-373, FAICS-773, FAICS-973, FAICS-1173.

Adsorbent	Temperature (K)	ΔG^o (kJ/mol)	ΔH^o (kJ/mol)	ΔS^o (J/mol K)	R^2
FAI	293	-7.09	2.80	-23.60	0.96
	313	-7.83			
	333	-8.44			
FAI-373	293	-7.22	1.37	-28.1	0.96
	313	-7.84			
	333	-8.39			
FAI-773	293	-6.90	1.17	-29.9	0.89
	313	-7.41			
	333	-8.01			
FAI-973	293	-6.87	2.34	-26.0	1.00
	313	-7.49			
	333	-8.13			
FAI-1173	293	-6.65	1.28	-30.40	0.99
	313	-7.20			
	333	-7.73			
FAICS-373	293	-7.60	2.38	-23,3	1.00
	313	-8.30			
	333	-8.96			
FAICS-773	293	-7.87	1.15	-26.7	0.89
	313	-8.45			
	333	-9.11			
FAICS-973	293	-7.96	1.72	-24.36	0.99
	313	-8.65			
	333	-9.28			
FAICS-1173	293	-7.70	2.27	-23.44	0.98
	313	-8.35			
	333	-9.06			